Helmholtz–Gauss waves

Julio C. Gutiérrez-Vega and Miguel A. Bandres

Photonics and Mathematical Optics Group, Tecnológico de Monterrey, Monterrey, México, 64849

Received June 23, 2004; revised manuscript received August 17, 2004; accepted August 18, 2004

A detailed study of the propagation of an arbitrary nondiffracting beam whose disturbance in the plane $z = 0$ is modulated by a Gaussian envelope is presented. We call such a field a Helmholtz–Gauss (HzG) beam. A simple closed-form expression for the paraxial propagation of the HzG beams is written as the product of three factors: a complex amplitude depending on the z coordinate only, a Gaussian beam, and a complex scaled version of the transverse shape of the nondiffracting beam. The general expression for the angular spectrum of the HzG beams is also derived. We introduce for the first time closed-form expressions for the Mathieu–Gauss beams in elliptic coordinates and for the parabolic Gauss beams in parabolic coordinates. The properties of the considered beams are studied both analytically and numerically. © 2005 Optical Society of America

OCIS codes: 260.1960, 350.5500, 140.3300, 050.1960.

1. INTRODUCTION

Nondiffracting beams have attracted attention ever since Durnin *et al.*[1,2] first reported the generation of the Bessel beams in 1987. In their original papers, Bessel beams were obtained as solutions to the homogeneous scalar wave equation expressed in circular cylindrical coordinates. Thereafter, several exact nondiffracting solutions of the wave equation have also been reported, for instance Mathieu beams in elliptic coordinates[3–5] and parabolic beams in parabolic coordinates.[6] The transverse intensity distribution of these ideal nondiffracting beams remains unchanged in free-space propagation.

Ideal nondiffracting beams have an infinite extent and energy, and thus they are not physically realizable. In view of this, some papers have been devoted to describing modified versions of Bessel beams, which carry finite energy and may be said to be nearly nondiffracting because they can propagate over a large range without significant divergence. In particular, Gori *et al.*[7] introduced in 1987 the Bessel–Gauss (BG) beams, i.e., Bessel beams apodized by a Gaussian transmittance, which carry a finite power and can be realized experimentally to a very good approximation.

The original BG beams have been generalized in a number of ways; for instance, Li *et al.*[8] studied the behavior of Bessel beams modulated by flat-topped Gaussian functions and suggested that beams with different transverse shapes and nondiffractinglike features can be expressed as a series of conventional BG beams of different orders. Kiselev[9] applied the separation-of-variables method to find a general expression for describing the propagation of a Gaussian beam whose amplitude is multiplied at a given plane by a function that is a solution of the two-dimensional Helmholtz equation. BG beams are thus a special case of the Kiselev solutions.

In this paper we present a rigorous and detailed study of the propagation of an arbitrary nondiffracting beam whose disturbance in the plane $z = 0$ is modulated by a Gaussian envelope. Because nondiffracting beams are solutions of the Helmholtz equation, we call such a field a Helmholtz–Gauss (HzG) beam. We derive a simple closed-form expression for the propagation of the HzG beams that can be written as the product of three factors: a complex amplitude depending on the z coordinate only, a Gaussian beam, and a complex scaled version of the transverse shape of the nondiffracting beam. Unlike ideal nondiffracting beams, HzG beams carry finite power and can be realized experimentally to a very good approximation. BG beams are a special case of HzG beams.

The general expression for the angular spectrum of the HzG beams is derived, and their properties discussed. We found that the angular spectrum of the HzG beam is represented by an annular ring in the frequency space. While the mean radius of the ring is defined exclusively by the transverse structure of the ideal nondiffracting beam, the width of the annulus is specified by the Gaussian envelope only.

We introduce for the first time closed-form expressions for the Mathieu–Gauss (MG) beams in elliptic coordinates and for the parabolic Gauss (PG) beams in parabolic coordinates. The behavior of the considered beams on propagation is studied both analytically and numerically. This work extends and consolidates the previous descriptions and generalizations of nondiffracting optical beams.

2. HELMHOLTZ–GAUSS BEAM

Let us suppose that a monochromatic wave $U(\mathbf{r})$ with time dependence $\exp(-i\omega t)$ has a disturbance across the plane $z = 0$ given by

$$U_0(\mathbf{r}_t) = \exp(-r^2/w_0^2) W(\mathbf{r}_t; k_t), \tag{1}$$

where $\mathbf{r}_t = (x, y) = (r, \phi)$ denotes the transverse coordinates, $W(\mathbf{r}_t; k_t)$ is the transverse pattern of an ideal nondiffracting beam $W(\mathbf{r}_t; k_t)\exp(ik_z z)$, and w_0 is the waist size of a Gaussian envelope. The transverse (k_t) and longitudinal (k_z) components of the wave vector $\mathbf{k}$ satisfy the relation $k^2 = k_t^2 + k_z^2$.

1084-7529/2005/020289-10$15.00

The transverse distribution $W(\mathbf{r}_t; k_t)$ of the ideal nondiffracting beam fulfills the two-dimensional Helmholtz equation

$$\left(\frac{\partial^2}{\partial x^2} + \frac{\partial^2}{\partial y^2} + k_t^2\right) W(\mathbf{r}_t; k_t) = 0 \tag{2}$$

and can be expressed as a superposition of plane waves whose transverse wave numbers k_t are restricted to a single value, that is,

$$W(\mathbf{r}_t; k_t) = \int_{-\pi}^{\pi} A(\varphi)\exp[ik_t(x\cos\varphi + y\sin\varphi)]\mathrm{d}\varphi, \tag{3}$$

where $A(\varphi)$ is the angular spectrum of the ideal nondiffracting beam. This angular spectrum is located on a single ring of radius $\rho = k_t$ in the frequency space.

The HzG field $U(\mathbf{r})$ can be determined in terms of its value $U_0(\mathbf{r}_t)$ at $z = 0$. By using the fact that nondiffracting beams can be expanded in terms of plane waves, we demonstrate in Appendix A that $U(\mathbf{r})$ is given by

$$U(\mathbf{r}) = \exp\left(-i\frac{k_t^2}{2k}\frac{z}{\mu}\right)\mathrm{GB}(\mathbf{r})W\left(\frac{x}{\mu}, \frac{y}{\mu}; k_t\right), \tag{4}$$

where $\mathrm{GB}(\mathbf{r})$ is the fundamental Gaussian beam

$$\mathrm{GB}(\mathbf{r}) = \frac{\exp(ikz)}{\mu}\exp\left(-\frac{r^2}{\mu w_0^2}\right) \tag{5}$$

and

$$\mu = \mu(z) = 1 + iz/z_R, \tag{6}$$

with $z_R = kw_0^2/2$ being the usual Rayleigh range of a Gaussian beam.[10] Equation (4) is a solution of the homogeneous Helmholtz equation under the paraxial regime throughout the whole space and reduces to Eq. (1) when it is evaluated in the plane $z = 0$. One thus notices that the propagation of a HzG beam gives rise to distinct longitudinal amplitude and aspheric phase factors.

While the arguments of the function W at the plane $z = 0$ are real, outside this plane they become complex i.e., $\bar{x} = x/\mu$ and $\bar{y} = y/\mu$, with the result that the initial shape defined by W may change its form dramatically on propagation. It is also worth noting that the function $W(\bar{x}, \bar{y}; k_t)$ still satisfies the two-dimensional Helmholtz equation

$$\left(\frac{\partial^2}{\partial \bar{x}^2} + \frac{\partial^2}{\partial \bar{y}^2} + k_t^2\right) W(\bar{x}, \bar{y}; k_t) = 0 \tag{7}$$

and admits the following integral representation:

$$W(\bar{x}, \bar{y}; k_t) = \int_{-\pi}^{\pi} A(\varphi)\exp[ik_t(\bar{x}\cos\varphi + \bar{y}\sin\varphi)]\mathrm{d}\varphi. \tag{8}$$

The angular spectrum of a HzG beam across a plane parallel to the (x, y) plane at a distance z from the origin is given by the two-dimensional Fourier transform

$$\mathfrak{U}(u, v; z) = \frac{1}{2\pi}\int\int U(x, y, z)\exp(-ixu - iyv)\mathrm{d}x\mathrm{d}y, \tag{9}$$

where (u, v) are the Cartesian coordinates in the frequency space and the double integral is carried out over the whole plane (x, y). By substituting Eq. (4) into Eq. (9), we show in Appendix B that the spectrum of the HzG beam is given by

$$\mathfrak{U}(u, v; z) = D(z)\exp\left(-\frac{w_0^2\mu}{4}\rho^2\right)W\left(\frac{w_0^2}{2i}u, \frac{w_0^2}{2i}v; k_t\right), \tag{10}$$

where $\rho = (u^2 + v^2)^{1/2}$ and

$$D(z) = \frac{w_0^2}{2}\exp\left(-\frac{1}{4}k_t^2 w_0^2\right)\exp(ikz) \tag{11}$$

is a complex amplitude factor that depends on z only.

3. PROPAGATION PROPERTIES OF HELMHOLTZ–GAUSS BEAMS

We will now discuss the general propagation properties of the HzG beam and its angular spectrum.

A. Helmholtz–Gauss Beam Behavior

From Eq. (4), it is straightforward to verify that when $w_0 \to \infty$, the HzG beam becomes

$$U(\mathbf{r}) = \exp[i(k - k_t^2/2k)z]W(\mathbf{r}_t; k_t), \tag{12}$$

which is indeed the equation of an ideal nondiffracting beam with the longitudinal wave vector k_z expressed in the paraxial approximation $k - k_t^2/2k$. On the other hand, from Eq. (8), we see that when k_t tends to zero, the function W becomes a constant and consequently the HzG beam reduces to a pure Gaussian beam.

Following the physical picture used by Gori *et al.*[7] to gain a basic understanding of the propagation features of the BG beams, one may imagine that a HzG beam is formed as a coherent superposition of fundamental Gaussian beams that have their waist planes coincident with the plane $z = 0$, whose mean propagation axes lie on the surface of a cone with a half-aperture angle $\theta_0 = \arcsin(k_t/k) \approx k_t/k$ and whose amplitudes are modulated angularly by the function $A(\varphi)$. The propagation characteristics are thereby governed by the spreading of the beam due to the conical propagation and the diffraction of the constituent Gaussian beams whose diffraction angle is $\theta_G = 2/kw_0$.[10]

The parameter

$$\gamma = \frac{\theta_0}{\theta_G} = \frac{1}{2}k_t w_0 \tag{13}$$

plays an important role in the propagation of the HzG beams. When $\gamma \gg 1$, a significant superposition of all the constituent Gaussian beams will survive up to a distance

$$z_{\max} = \frac{w_0}{\sin\theta_0} \approx \frac{w_0 k}{k_t} = \frac{z_R}{\gamma}. \tag{14}$$

This is a conservative estimate because the spot size of the Gaussian beams actually increases along the propagation axis. For $\gamma \gg 1$ the HzG beam retains the nondiffracting propagation properties of the ideal nondiffracting beam within the range $z \in [-z_{\max}, z_{\max}]$. Outside this zone, the HzG beam will diverge and acquire wave-front curvature, forming a ring-shaped far-field pattern with mean radius $z \tan \theta_0$, an angular variation given approximately by $A(\varphi)$, and leaving the central region near the z axis practically obscure.

The case $\gamma \ll 1$ occurs when $\lambda_t = (2\pi/k_t) \gg \pi w_0$; thus the outer radial oscillations of the function W at the plane $z = 0$ are strongly damped, leaving only a Gaussian-like spot that is angularly modulated by the azimuthal dependence of the ideal nondiffracting beam. The case $\gamma \sim 1$ corresponds to the transition zone between the Gaussian-like behavior ($\gamma \ll 1$) and the nondiffractinglike behavior ($\gamma \gg 1$).

B. Axial Irradiance Distribution

By setting $r = 0$ in Eq. (4), we can obtain the normalized axial irradiance distribution $I(z) = |U(0, 0, z)|^2/|W(0, 0)|^2$ of the HzG beams, namely,

$$I(\bar{z}) = \frac{1}{1 + \bar{z}^2} \exp\left(-\frac{2\gamma^2 \bar{z}^2}{1 + \bar{z}^2} \right), \tag{15}$$

where $\bar{z} = z/z_R$ is the normalized propagation distance. Equation (15) can be applied only to beams for which the field at the origin does not vanish. The irradiance distribution as a function of z is depicted in Fig. 1 for $\gamma = 1,3,...,15$. For each curve, the vertical dashed line is located at the maximum distance $z_{\max} = (2k/k_t^2)\gamma$ [see Eq. (14)], for which the axial irradiance assumes the value

$$I(z_{\max}) = \frac{\gamma^2}{1 + \gamma^2} \exp\left(-\frac{2\gamma^2}{1 + \gamma^2} \right). \tag{16}$$

Note that the axial irradiance of the HzG beams is a monotonically decreasing function of the propagation distance z, and consequently it does not present axial irradiance oscillations, as occurs for apertured ideal nondiffracting beams.[1,8]

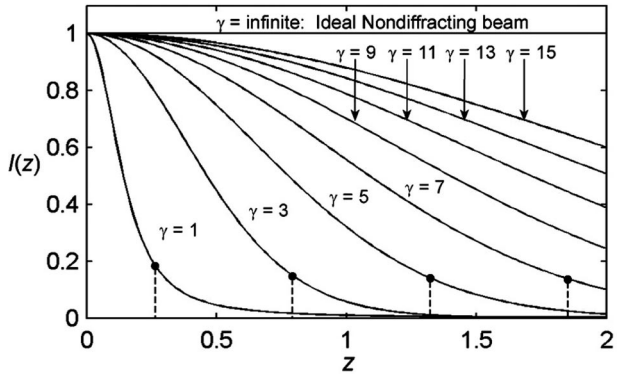

Fig. 1. Normalized axial irradiance distribution of a HzG beam as a function of z for $\gamma = 1,3,...,15$. The vertical dashed lines are located at the maximum distance $z_{\max} = z_R/\gamma$. For numerical purposes, $\lambda = 632.8$ nm and $\theta_0 = 0.05°$.

C. Angular Spectrum Behavior

The angular spectrum of the HzG beams also exhibits an interesting dependence on the parameter γ. In Appendix B, we show that the angular spectrum [Eq. (10)] comes from the azimuthal superposition of waves whose radial dependence can be written in the form

$$\exp\left(-\frac{w_0^2 \mu}{4} \rho^2 \right) \exp\left(\frac{k_t w_0^2}{2} \rho \right) \tag{17}$$

[see Eq. (B4)]. The amplitude of the last expression is given by

$$\exp(\gamma^2) \exp\left[-\frac{1}{4} w_0^2 (\rho - k_t)^2 \right], \tag{18}$$

which is identified as a Gaussian function whose maximum is shifted a distance k_t from $\rho = 0$ and whose half-width is $2/w_0$. It is clear that for $\gamma \gg 1$ the angular spectrum of the HzG beam is represented by an annular ring in the frequency space. The mean radius of the ring is k_t, and consequently it is defined exclusively by the function W associated with the ideal nondiffracting beam. On the other hand, the width of the ring is $4/w_0$; it is thus defined by only the Gaussian envelope. It is instructive to see that a scaling of the transverse dimensions of the nondiffracting beam W changes only the middle radius of the ring, whereas its width remains unchanged.

When $w_0 \to \infty$, the HzG can be approximated by an ideal nondiffracting beam, expression (18) tends to a delta function $\delta(\rho - k_t)$, and the angular spectrum becomes a δ-like ring of radius k_t over the plane (u, v). On the other hand, in the case of HzG beams for which the field at the origin does not vanish, the Gaussian function $\exp(-r^2/w_0^2)$ becomes a very narrow impulse function at $r = 0$ when $w_0 \to 0$, and consequently the HzG beam in the plane $z = 0$ behaves as a bright point source at the origin, expression (18) tends to a constant, and the power spectrum is practically independent of the radius ρ. Finally, we note from Eq. (10) that the transverse structure of the power spectrum $|\mathfrak{U}(u, v; z)|^2$ remains invariant under propagation, i.e., $|\mathfrak{U}(u, v; z)|^2 = |\mathfrak{U}(u, v; 0)|^2$.

4. FOUR FAMILIES OF HELMHOLTZ–GAUSS BEAMS

In Section 3, the general propagation properties of the HzG beams were discussed. Particular attention was focused on the behavior of the beam and the angular spectrum. In this section, we investigate the propagation characteristics of the HzG beams corresponding to each fundamental family of ideal nondiffracting beams; they are plane waves in Cartesian coordinates, Bessel beams in circular cylindrical coordinates,[1,2] Mathieu beams in elliptic cylindrical coordinates,[3–5] and parabolic beams in parabolic cylindrical coordinates.[6] We use the term "fundamental" to refer to a family of ideal nondiffracting beams that are eigenmodes of the Helmholtz equation in a cylindrical orthogonal coordinate system. A fundamental family constitutes a basis for expanding any nondiffracting beam with the same transverse spatial frequency k_t. As far as we know, the general analytical expressions for the Mathieu–Gauss (MG) beams and parabolic

Gauss (PG) beams have not been reported nor have their propagation features been studied in the literature.

A. Cosine Gauss Beams

One of the simplest nondiffracting beams in Cartesian coordinates is the ideal cosine field

$$W(\mathbf{r}_t;\, k_t) = \cos(k_t y) \tag{19}$$

resulting from the superposition of two ideal plane waves $\exp(ik_t y)/2 + \exp(-ik_t y)/2$. Its angular spectrum is not continuous but discrete, namely, $A(\varphi) = \delta(\varphi - \pi/2) + \delta(\varphi + \pi/2)$, where $\delta(\cdot)$ is the Dirac delta function. The cosine field (19) can be easily produced in the laboratory with a two-point Young experiment.

When the general expression for a HzG beam [Eq. (4)] is applied, the expression for a cosine Gauss (CG) beam is given by

$$\mathrm{CG}(\mathbf{r}) = \exp\left(-i\,\frac{k_t^2}{2k}\,\frac{z}{\mu}\right)\mathrm{GB}(\mathbf{r})\cos\left(\frac{k_t y}{\mu}\right). \tag{20}$$

Despite its simplicity, the CG beam exhibits all the propagation characteristics of a HzG beam. The transverse amplitude distribution of a CG beam is shown in Figs. 2(a), 2(b), and 2(c) for $z/z_{\max} = 0$, 0.6, and 1.2, respectively. For numerical purposes, we chose a waist spot $w_0 = 2$ mm and the parameter $\gamma = 10$. Assuming an illumination at wavelength $\lambda = 632.8$ nm produces $k_t = 10{,}000\ \mathrm{m}^{-1}$ and $z_{\max} \approx 1.98$ m. At the plane $z = 0$, the field reduces to $\exp(-r^2/w_0^2)\cos(k_t y)$.

The propagation of the amplitude and phase profiles of a CG beam along the planes (y, z) and (x, z) are depicted in Figs. 2(d) and 2(e). These plots were obtained by evaluating Eq. (20) at 201 transverse planes evenly spaced throughout the interval $[-1.2z_{\max}, 1.2z_{\max}]$. The CG beam behaves like a nondiffracting cosine field within the range $|z| \leqslant z_{\max}$.

The angular spectrum of the CG beam is determined directly from Eqs. (10) and (19); after using the identity $\cos(\pm ix) = \cosh(x)$, we obtain

$$\mathfrak{CG}(u, v; z) = D(z)\exp\left(-\frac{\mu w_0^2}{4}\rho^2\right)\cosh[2\gamma^2(v/k_t)]. \tag{21}$$

The amplitude and phase distribution of the angular spectrum is plotted as a function of the normalized spatial frequencies in Figs. 2(f)–2(h) for $z = 0.6z_{\max}$ and $1.2z_{\max}$. The transverse shape of the power spectrum $|\mathfrak{CG}(u, v; z)|^2$ is invariant under propagation. As expected, the angular spectrum of the CG beam is represented by two Gaussian-like spots placed at $(u, v) = (0, \pm k_t)$ and whose half-width is $2/w_0$.

B. Bessel–Gauss Beams

The BG beams have been studied elsewhere[7,8]; in this subsection, we briefly discuss them for completeness.

Bessel beams are exact nondiffracting solutions of the scalar wave equation in circular cylindrical coordinates.[1,2] The transverse field of the mth-order Bessel beam reads as

$$W(\mathbf{r}_t;\, k_t) = J_m(k_t r)\exp(im\phi), \tag{22}$$

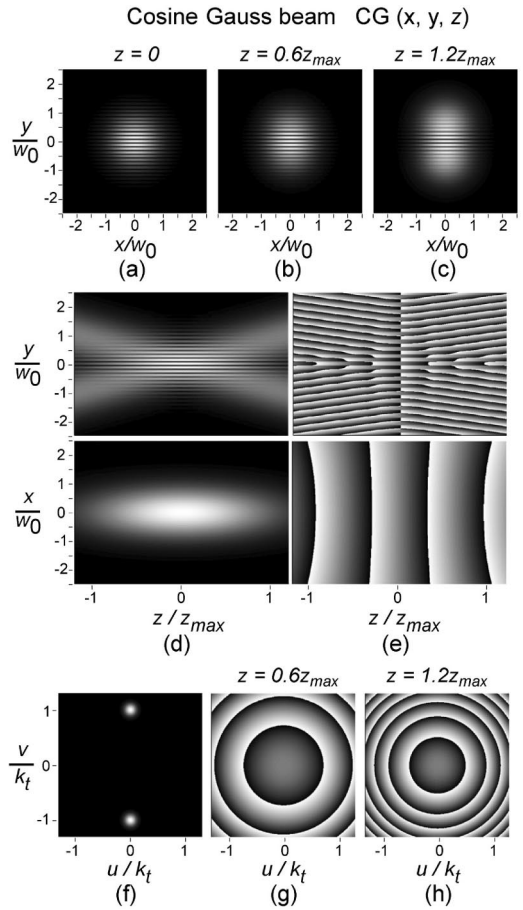

Fig. 2. (a)–(c) Transverse amplitude distribution of a CG beam at different z planes; (d), (e) propagation of the amplitude and phase profiles along the planes (y, z) and (x, z); (f)–(h) amplitude and phase distribution of the angular spectrum at different z planes.

where $J_m(\cdot)$ is the mth-order Bessel function. The angular spectrum of the Bessel beams is located on a single ring of radius $\rho = k_t$ in the frequency space, and its angular dependence is $A(\varphi) \propto \exp(im\varphi)$.

Applying Eq. (4) and also noting that $(x/\mu, y/\mu) \rightarrow (r/\mu, \phi)$, we find the expression for the BG beams to be

$$\mathrm{BG}_m(\mathbf{r}) = \exp\left(-i\,\frac{k_t^2}{2k}\,\frac{z}{\mu}\right)\mathrm{GB}(\mathbf{r})J_m\left(\frac{k_t r}{\mu}\right)\exp(im\phi), \tag{23}$$

which is fully equivalent to other expressions for BG beams analyzed previously.[7–9]

The transverse amplitude distribution of a first-order BG beam is shown in Figs. 3(a), 3(b), and 3(c) for $z/z_{\max} = 0$, 0.6, and 1.2, respectively. For numerical purposes, we chose a waist spot $w_0 = 3$ mm and the parameter $\gamma = 13$. Assuming an illumination at wavelength $\lambda = 632.8$ nm produces $k_t = 8665\ \mathrm{m}^{-1}$ and $z_{\max} \approx 3.44$ m. The propagation of the amplitude and phase profiles along the plane (y, z) are depicted in Fig. 3(d). These plots were obtained by evaluating Eq. (23) at 201 transverse planes evenly spaced throughout the interval $[-1.2z_{\max}, 1.2z_{\max}]$. Outside this zone, the BG beam di-

verges, forming a ring-shaped pattern with mean radius $z \tan \theta_0$, where the half-aperture angle is $\theta_0 = \arcsin(k_t/k) = 0.05°$.

The angular spectrum of the BG beams is determined directly from Eqs. (10) and (22); after using the identity $J_m(-ix) = (-i)^m I_m(x)$, we obtain

$$\mathfrak{BG}_m(u, v; z) = (-i)^m D(z) \exp\left(-\frac{\mu w_0^2}{4}\rho^2\right) I_m(2\gamma^2\rho/k_t) \times \exp(im\phi), \tag{24}$$

where $I_m(\cdot)$ is the mth-order modified Bessel function of the first kind.

C. Mathieu–Gauss Beams

Recently, Gutiérrez-Vega *et al.*[3–5] demonstrated theoretically and experimentally the existence of the third family of nondiffracting beams resulting from the solution of the wave equation in elliptic cylindrical coordinates. Since the transverse pattern of such beams is described by the Mathieu functions, they were called Mathieu beams. The exact analytical expression for the MG beams of any order has not been reported yet.

The elliptic coordinates (ξ, η) are defined by $x = f\cosh\xi\cos\eta$ and $y = f\sinh\xi\sin\eta$, where $\xi \in [0, \infty)$ and $\eta \in [0, 2\pi)$ are the radial and angular variables, respectively, and $2f$ is the interfocal separation. The transverse field of the mth-order even and odd Mathieu beams are written as

$$W^e(\mathbf{r}_t; k_t) = \mathrm{Je}_m(\xi, q)\mathrm{ce}_m(\eta, q), \tag{25a}$$

$$W^o(\mathbf{r}_t; k_t) = \mathrm{Jo}_m(\xi, q)\mathrm{se}_m(\eta, q), \tag{25b}$$

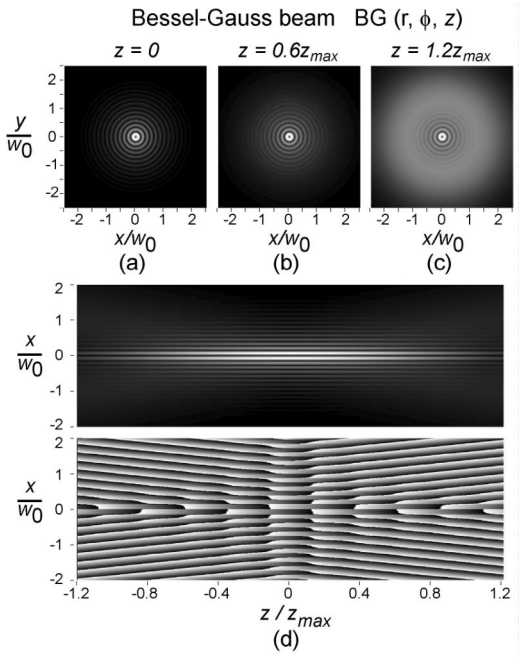

Fig. 3. (a)–(c) Transverse amplitude distribution of a first-order BG beam at different z planes, (d) propagation of the amplitude and phase profiles along the plane (x, z) in the range $[-1.2z_{\max}, 1.2z_{\max}]$.

where $\mathrm{Je}_m(\cdot)$ and $\mathrm{Jo}_m(\cdot)$ are the mth-order even and odd modified Mathieu functions, respectively, and $\mathrm{ce}_m(\cdot)$ and $\mathrm{se}_m(\cdot)$ are the mth-order even and odd ordinary Mathieu functions, respectively.[11] The parameter $q = f^2k_t^2/4$ carries information about the transverse spatial frequency k_t and the ellipticity of the coordinate system through f. The angular spectra of the even and odd Mathieu beams lie on a ring of radius $\rho = k_t$ in the frequency space, and their angular variations are given by $A^e(\varphi) \propto \mathrm{ce}_m(\varphi, q)$ and $A^o(\varphi) \propto \mathrm{se}_m(\varphi, q)$, respectively.

From Eqs. (4) and (25a), the closed-form expression for the propagation of the mth-order even MG beams is found to be

$$\mathrm{MG}_m^e(\mathbf{r}) = \exp\left(-i\frac{k_t^2}{2k}\frac{z}{\mu}\right)\mathrm{GB}(\mathbf{r})\mathrm{Je}_m(\bar{\xi}, q)\mathrm{ce}_m(\bar{\eta}, q), \tag{26}$$

where in a transverse z plane the complex elliptic variables $(\bar{\xi}, \bar{\eta})$ are determined by the relations

$$x = f_0(1 + iz/z_R)\cosh\bar{\xi}\cos\bar{\eta}, \tag{27a}$$

$$y = f_0(1 + iz/z_R)\sinh\bar{\xi}\sin\bar{\eta}, \tag{27b}$$

with f_0 being the semifocal separation at the waist plane $z = 0$. Note that, while the elliptic variables $(\bar{\xi}, \bar{\eta})$ at the plane $z = 0$ are real, outside this plane they become complex in order to satisfy the requirement that the Cartesian coordinates (x, y) remain real in the entire space. MG beams of the form (26) constitute a complete family of paraxial fields in the sense that any HzG beam with the same k_t can be expressed as a superposition of MG beams with the appropriate weight factors.

The transverse amplitude distribution of a second-order even MG beam with $q = 16$ is shown in Figs. 4(a), 4(b), and 4(c) for $z/z_{\max} = 0$, 0.6, and 1.2, respectively. We chose a waist spot $w_0 = 3$ mm and a transverse wave number for the Mathieu beam given by $k_t = 8000\,\mathrm{m}^{-1}$. Assuming an illumination at wavelength $\lambda = 632.8$ nm produces $\gamma = 12$, $z_{\max} \approx 3.72$ m, and $f_0 = 1$ mm. The propagation of the amplitude profiles along the planes (y, z) and (x, z) is depicted in Fig. 4(d). These plots were obtained by evaluating Eq. (26) at 101 transverse planes evenly spaced throughout the interval $[0, 1.2z_{\max}]$. Note the characteristic cone-shaped region where constituent waves superpose to build up the MG beam. The MG beam behaves like a nondiffracting Mathieu beam within the range $|z| \leqslant z_{\max}$.

The angular spectrum of the MG beams is obtained directly from Eqs. (10) and (26); we have

$$\mathfrak{MG}_m^e(u, v; z) = D(z)\exp\left(-\frac{\mu w_0^2}{4}\rho^2\right)\mathrm{Je}_m(\hat{\xi}, q)\mathrm{ce}_m(\hat{\eta}, q), \tag{28}$$

where the complex elliptic variables $(\hat{\xi}, \hat{\eta})$ in the frequency space are determined by the following relations:

$$u = \frac{2i}{w_0^2} f_0 \cosh\hat{\xi}\cos\hat{\eta}, \tag{29a}$$

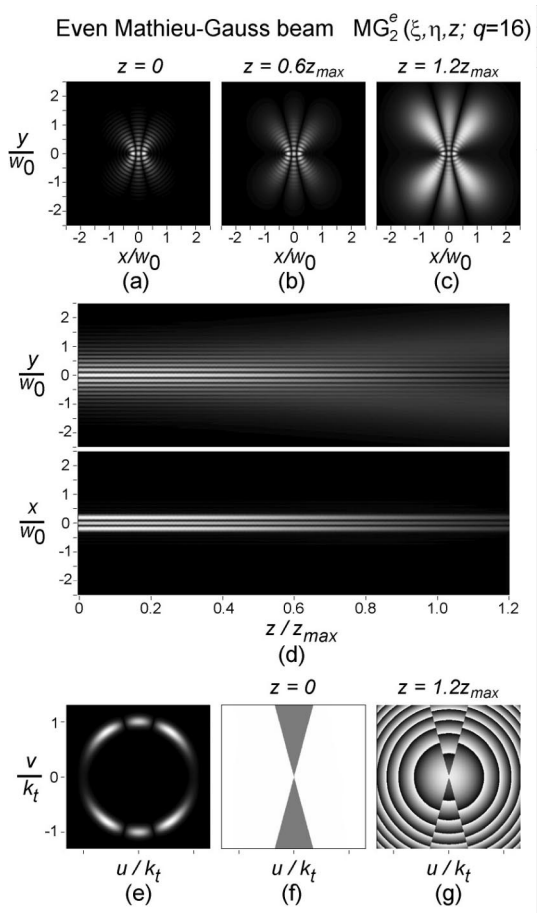

Fig. 4. (a)–(c) Transverse amplitude distribution of a second-order even MG beam at different z planes, (d) propagation of the amplitude pattern along the planes (y, z) and (x, z) in the range $[0, 1.2z_{\max}]$, (e)–(g) amplitude and phase distributions of the angular spectrum as a function of the normalized coordinates $(u/k_t, v/k_t)$.

$$v = \frac{2i}{w_0^2} f_0 \sinh\hat{\xi} \sin\hat{\eta}. \tag{29b}$$

The amplitude and phase distributions of the spectrum of the MG_2^e beam are shown in Figs. 4(e)–4(g) as a function of the normalized coordinates $(u/k_t, v/k_t)$ for $z = 0$ and $1.2z_{\max}$. The transverse shape of the power spectrum $|\mathfrak{MG}_m^e(u, v; z)|^2$ is invariant under propagation. As expected, for $\gamma = 12$ the angular spectrum is an azimuthally modulated annular ring with mean radius $\rho/k_t = 1$ and angular dependence approximately given by $\mathrm{ce}_2(\varphi, q)$.

BG beams with azimuthal angular dependence $\exp(im\phi)$ have a phase that rotates circularly around the propagation axis. In a similar way, from the stationary mode solutions described by Eq. (26), it is possible to construct helical Mathieu–Gauss (HMG) beams of the form

$$\mathrm{HMG}_m^{\pm}(\mathbf{r}) = \mathrm{MG}_m^e(\mathbf{r}) \pm i\mathrm{MG}_m^o(\mathbf{r}), \tag{30}$$

but whose phase rotates now elliptically around a strip defined by $(|x| \leqslant f, 0, z)$. The sign in Eq. (30) defines the rotating direction. Equation (30) is valid for $m > 0$ because $\mathrm{MG}_m^o(\mathbf{r})$ is not defined for $m = 0$. In Figs. 5(a), 5(b), and 5(c), we show the transverse magnitudes and phases of the helical modes $\mathrm{HMG}_7^{\pm}(\mathbf{r}; q = 16)$ at planes $z = 0$, $0.6z_{\max}$, and $1.2z_{\max}$, respectively. The pattern consists of well-defined elliptic confocal rings with a dark elliptic spot on axis. The amplitude and phase distribution of the spectrum of $\mathrm{HMG}_7^{\pm}(\mathbf{r}; q = 16)$ is shown in Figs. 5(d)–5(f) for $z = 0$ and $z = 1.2z_{\max}$. The HMG beams presented here could be applied to construct elliptic optical tweezers and atom traps as well to study the transfer of angular momentum to microparticles or atoms.

D. Parabolic Gauss Beams

In a recent paper, Bandres *et al.*[6] demonstrated theoretically the existence of parabolic beams, which constitute the fourth family of fundamental nondiffracting beams. It was found that the transverse structure of the parabolic beams is described by the parabolic functions, and, contrary to Bessel or Mathieu beams, their eigenvalue is continuous instead of discrete. In this subsection, we introduce for the first time a closed-form expression for the PG beams.

The parabolic cylindrical coordinates (ξ, η) are defined by $x = (\eta^2 - \xi^2)/2$ and $y = \xi\eta$, where the variables ranges in $\xi \in [0, \infty)$ and $\eta \in (-\infty, \infty)$. The transverse field of the even and odd parabolic beams is written as

$$W^e(\xi, \eta; k_t) = \frac{|\Gamma_1|^2}{\pi\sqrt{2}} \mathrm{P}_e(\sqrt{2k_t}\xi; a)\mathrm{P}_e(\sqrt{2k_t}\eta; -a), \tag{31a}$$

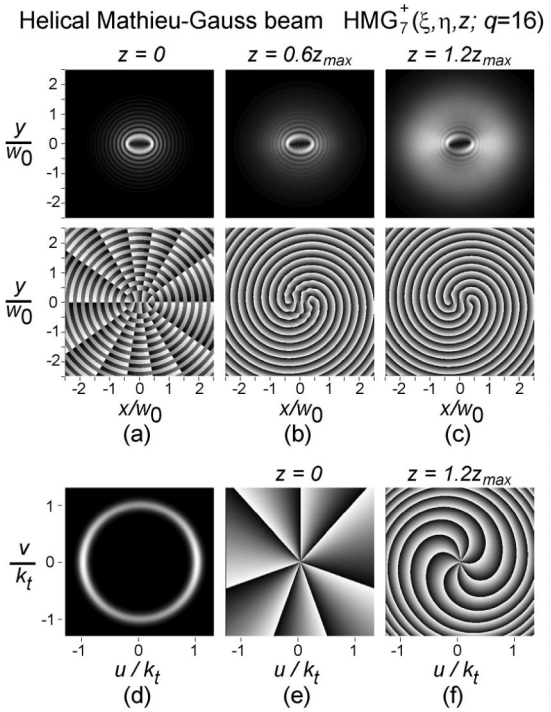

Fig. 5. (a)–(c) Transverse amplitude and phase distributions of a seventh-order HMG beam at different z planes, (d)–(f) amplitude and phase distributions of the angular spectrum as a function of the normalized coordinates $(u/k_t, v/k_t)$.

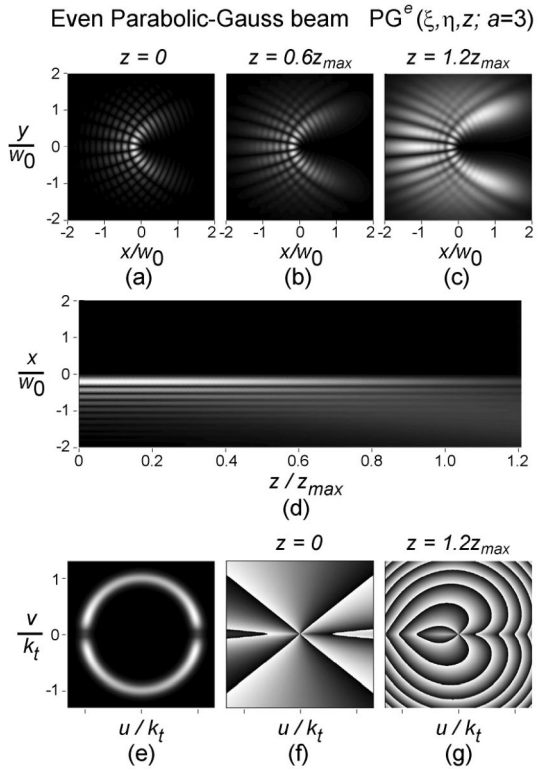

Fig. 6. (a)–(c) Transverse amplitude distribution of an even PG beam with $a = 3$ at different z planes, (d) propagation of the amplitude pattern along the plane (x, z) in the range $[0, 1.2z_{\max}]$, (e)–(g) amplitude and phase distributions of the angular spectrum.

$$W^o(\xi,\ \eta;\ k_t) = \frac{|\Gamma_3|^2}{\pi\sqrt{2}} \mathrm{P}_o(\sqrt{2k_t}\xi;\ a)\mathrm{P}_o(\sqrt{2k_t}\eta;\ -a), \tag{31b}$$

where $\Gamma_1 = \Gamma(\frac{1}{4} + \frac{1}{2}ia)$, $\Gamma_3 = \Gamma(\frac{3}{4} + \frac{1}{2}ia)$, and the parameter a represents the order of the beam and can assume any real value in the range $(-\infty, \infty)$. The functions $\mathrm{P}_e(\cdot)$ and $\mathrm{P}_o(\cdot)$ are the even and odd solutions to the parabolic cylindrical differential equation $[\mathrm{d}^2/\mathrm{d}x^2 + (x^2/4 - a)]\mathrm{P}(x;\ a) = 0$. The angular spectrum of the even parabolic beams lies on a ring of radius $\rho = k_t$ in the frequency space, and its angular variation is given by $A^e(\varphi) = (4\pi|\sin\varphi|)^{-1/2}\exp[ia\ln|\tan(\varphi/2)|]$.

Applying Eq. (4) and also noting that $(x/\mu, y/\mu) \rightarrow (\xi/\sqrt{\mu},\ \eta/\sqrt{\mu})$ for parabolic coordinates, we find the expression for the even PG beams, $\mathrm{PG}^e(\mathbf{r})$ to be

$$\mathrm{PG}^e(\mathbf{r};\ a) = \exp\left(-i\frac{k_t^2}{2k}\frac{z}{\mu}\right)\mathrm{GB}(\mathbf{r})\frac{|\Gamma_1|^2}{\pi\sqrt{2}} \times \mathrm{P}_e(\sqrt{2k_t/\mu}\xi;\ a)\mathrm{P}_e(\sqrt{2k_t/\mu}\eta;\ -a). \tag{32}$$

The transverse amplitude distribution of an even PG beam with $a = 3$ is shown in Figs. 6(a), 6(b), and 6(c) for $z/z_{\max} = 0$, 0.6, and 1.2, respectively. The field exhibits well-defined parabolic nodal lines. We chose a waist size of the Gaussian modulation given by $w_0 = 2$ mm and the parameter $\gamma = 10$. Assuming an illumination at wavelength $\lambda = 632.8$ nm produces $k_t = 10{,}000\ \mathrm{m}^{-1}$ and $z_{\max} \approx 1.98$ m. The propagation of the amplitude profile along the plane (x, z) is depicted in Fig. 6(d). This plot was obtained by evaluating Eq. (32) at 101 transverse planes evenly spaced throughout the interval $[0, 1.2z_{\max}]$. PG beams of the form (32) constitute a complete family of paraxial fields in the sense that any HzG beam with the same k_t and w_0 can be expressed as a superposition of PG beams with the appropriate weight factors.

The angular spectrum of the PG beams is obtained directly from Eqs. (10) and (31a); we have

$$\mathfrak{PG}^e(u,\ v;\ z) = D(z)\exp\left(-\frac{\mu w_0^2}{4}\rho^2\right)\frac{|\Gamma_1|^2}{\pi\sqrt{2}} \times \mathrm{P}_e(\sqrt{-ik_t w_0^2}\tilde{\xi};\ a)\mathrm{P}_e(\sqrt{-ik_t w_0^2}\tilde{\eta};\ -a), \tag{33}$$

where the parabolic coordinates $(\tilde{\xi},\ \tilde{\eta})$ in the frequency space are given by $u = (\tilde{\eta}^2 - \tilde{\xi}^2)/2$ and $v = \tilde{\xi}\tilde{\eta}$. The amplitude and phase distributions of the spectrum of the $\mathrm{PG}^e(\mathbf{r})$ beam are shown in Figs. 6(e)–6(g) as a function of the normalized coordinates $(u/k_t, v/k_t)$ for $z = 0$ and $1.2z_{\max}$. As expected, for $\gamma = 10$ the pattern of the spectrum is a ring with mean radius $\rho/k_t = 1$ and angular dependence approximately given by $A^e(\varphi)$.

From the stationary beam solutions described by Eqs. (32), it is possible to construct traveling PG (TPG) solutions of the form

$$\mathrm{TPG}^{\pm}(\mathbf{r};\ a) = \mathrm{PG}^e(\mathbf{r};\ a) \pm i\mathrm{PG}^o(\mathbf{r};\ a), \tag{34}$$

whose associated spectra are $A^{\pm}(\varphi;\ a) = A_e(\varphi;\ a) \pm iA_o(\varphi;\ a)$, in which the sign defines the traveling di-

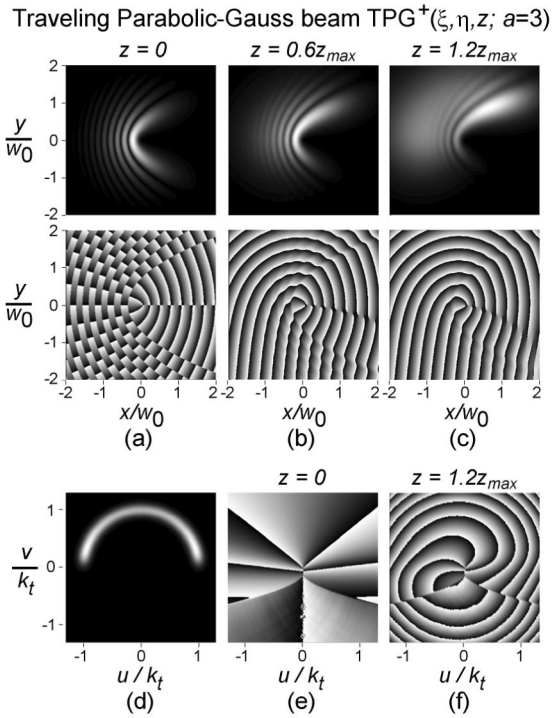

Fig. 7. (a)–(c) Transverse amplitude and phase distributions of a TPG beam with $a = 3$ at different z planes, (d)–(f) amplitude and phase distributions of the angular spectrum.

rection. In Figs. 7(a)–7(c), we show the transverse magnitudes and phases of the traveling $\mathrm{TPG}^{+}(\mathbf{r};\, a = 3)$ at planes $z = 0$, $0.6z_{\max}$, and $1.2z_{\max}$, respectively. The pattern consists of well-defined confocal parabolas opening along the positive x axis. The amplitude and phase distribution of the spectrum of $\mathrm{TPG}^{+}(\mathbf{r};\, a = 3)$ is shown in Figs. 7(d)–7(f) for $z = 0$ and $z = 1.2z_{\max}$. The traveling-wave feature can be observed in the gradient of their phase structure.

5. CONCLUSIONS

A detailed analysis of the propagation of an arbitrary nondiffracting beam whose disturbance in the plane $z = 0$ is modulated by a Gaussian envelope has been presented. We have found that the propagation through the whole space can be described by a simple and elegant closed-form expression composed of an amplitude factor depending on the z coordinate, a Gaussian beam, and a scaled version of the transverse shape of the ideal nondiffracting beam. Independently of the transverse shape of the ideal nondiffracting beam, our analysis revealed the existence of general features of the Helmholtz–Gauss (HzG) beams; for instance, the finite region where the beam exhibits a nondiffracting behavior, the doughnutlike far-field pattern, and the annular distribution of the angular spectrum. The transverse structure of the power spectrum remains invariant under propagation.

Closed-form expressions for the four families of HzG beams have been derived. In particular, we have discussed analytically and numerically for the first time the propagation properties of the Mathieu–Gauss beams in elliptic coordinates and the parabolic Gauss beams in parabolic coordinates.

APPENDIX A: DERIVATION OF THE HELMHOLTZ–GAUSS BEAM

While Gori *et al.*[7] and Li *et al.*[8] derived the BG beam solutions from the Kirchhoff–Huygens field integral under the Fresnel approximation starting from the disturbance at plane $z = 0$, Kiselev[9] applied the separation-of-variables technique to generalize the BG solutions. In this appendix, we follow a different approach to derive the analytical expression for a general HzG beam.

Ideal monochromatic nondiffracting beams can be obtained as a suitable superposition of plane waves whose transverse wave numbers k_t are restricted to a single value [see Eq. (3)]. With this in mind, we first investigate the propagation along the positive z axis of a tilted single plane wave $\exp[i(k_x x + k_y y + k_z z)]$, whose amplitude at the plane $z = 0$ is modulated by a Gaussian function, namely,

$$u_0(x, y) = \exp(-r^2/w_0^2)\exp[i(k_x x + k_y y)]. \tag{A1}$$

Let the field

$$u(\mathbf{r}) = \exp(ikz)\Psi(\mathbf{r}) \tag{A2}$$

satisfy the three-dimensional Helmholtz equation $(\nabla^2 + k^2)u(\mathbf{r}) = 0$ under the paraxial regime and restricted to the boundary condition $u(x, y, 0) = u_0(x, y)$. The function $\Psi(\mathbf{r})$ is a slowly varying complex envelope that satisfies the paraxial wave equation

$$\left(\frac{\partial^2}{\partial x^2} + \frac{\partial^2}{\partial y^2} + 2ik\frac{\partial}{\partial z}\right)\Psi(\mathbf{r}) = 0. \tag{A3}$$

We try to construct a solution of Eq. (A3) having the form

$$\Psi(\mathbf{r}) = \exp[iP(z)]\exp\left[\frac{ikr^2}{2q(z)}\right]\exp\left\{i\left[\frac{k_x x}{\mu(z)} + \frac{k_y y}{\mu(z)}\right]\right\}, \tag{A4}$$

where $\mu(z)$, $P(z)$, and $q(z)$ are functions to be determined. In assuming a solution of the form (A4), we are allowing for the possibility that the amplitude and the phase of the plane wave can vary with distance of propagation. Substitution of Eq. (A4) into the paraxial wave equation (A3) yields three equations

$$\frac{\mathrm{d}q}{\mathrm{d}z} - 1 = 0, \tag{A5a}$$

$$q\frac{\mathrm{d}\mu}{\mathrm{d}z} - \mu = 0, \tag{A5b}$$

$$i2k\mu^2 - k_t^2 q - 2kq\mu^2\frac{\mathrm{d}P}{\mathrm{d}z} = 0. \tag{A5c}$$

Integrating Eq. (A5a), we obtain

$$q = q_0 + z, \tag{A6}$$

where q_0 is a constant. Then Eq. (A5b) can be solved:

$$\mu = \mu_0 q, \tag{A7}$$

where μ_0 is a constant. If we substitute μ and q into Eq. (A5c), the function P is obtained after integration:

$$P = i\ln q + \frac{k_t^2}{2k\mu_0^2 q} + P_0, \tag{A8}$$

where P_0 is another constant to be determined.

The constants q_0, μ_0, and P_0 are determined by the requirement that $u(\mathbf{r})$, given by Eq. (A4) for $z = 0$, reduce to the boundary condition (A1), with the result that

$$q_0 = -iz_R, \quad \mu_0 = \frac{i}{z_R}, \quad P_0 = -i\ln(-iz_R) + i\frac{k_t^2 z_R}{2k}, \tag{A9}$$

where $z_R = kw_0^2/2$ is the Rayleigh range of the Gaussian beam. It then follows that

$$q(z) = z - iz_R, \tag{A10a}$$

$$\mu(z) = iq/z_R = 1 + iz/z_R, \tag{A10b}$$

$$P(z) = i\ln[(1 + z^2/z_R^2)^{1/2}] - \arctan\left(\frac{z}{z_R}\right) - \frac{k_t^2 z_R}{2k}\left(\frac{z_R}{q} - i\right). \tag{A10c}$$

Inserting $\mu(z)$, $P(z)$, and $q(z)$ into the field $\Psi(\mathbf{r})$ [Eq. (A4)], we obtain

$$\Psi(\mathbf{r}) = \exp\left(i\left\{ i\ln[(1+z^2/z_R^2)^{1/2}] - \arctan\left(\frac{z}{z_R}\right) - \frac{k_t^2 z_R}{2k}\left(\frac{z_R}{q}+i\right)\right\}\right) \times \exp\left[\frac{ikr^2}{q(z)}\right]\exp\left[i\left(\frac{k_x x}{\mu}+\frac{k_y y}{\mu}\right)\right]. \tag{A11}$$

By defining the constant $\kappa = k_t^2/2k$ and noting that $w(z) = w_0(1+z^2/z_R^2)^{1/2}$ and

$$\frac{1}{\mu} = \frac{1}{1+iz/z_R} = \frac{z_R}{iq} = \frac{w_0}{w(z)}\exp[-i\arctan(z/z_R)], \tag{A12}$$

we can write the field $\Psi(\mathbf{r})$ in the form

$$\Psi(\mathbf{r}) = \frac{1}{\mu}\exp\left(-i\frac{\kappa z}{\mu}\right)\exp\left(-\frac{r^2}{\mu w_0^2}\right)\exp\left[i\left(\frac{k_x x}{\mu}+\frac{k_y y}{\mu}\right)\right]. \tag{A13}$$

By multiplying by the longitudinal phase factor $\exp(ikz)$, we get

$$u(\mathbf{r}) = \exp\left(-i\frac{\kappa z}{\mu}\right)\frac{\exp(ikz)}{\mu} \times \exp\left(-\frac{r^2}{\mu w_0^2}\right)\exp\left[i\left(\frac{k_x x}{\mu}+\frac{k_y y}{\mu}\right)\right]. \tag{A14}$$

Equation (A14) describes the propagation of a tilted Gaussian wave whose mean wave vector has a projection $k_t = (k_x^2 + k_y^2)^{1/2}$ on the plane $z = 0$, forming an angle $\varphi = \arctan(k_y/k_x)$ with respect to the x axis.

HzG beams with arbitrary transverse distribution can be constructed by superposing waves of the form (A14), namely,

$$U(\mathbf{r}) = \int_{-\pi}^{\pi} A(\varphi)u(\mathbf{r})\mathrm{d}\varphi, \tag{A15}$$

where $A(\varphi)$ defines the amplitude and phase factor of the constituent Gaussian waves. Substituting Eq. (A14) into Eq. (A15), we obtain

$$U(\mathbf{r}) = \exp\left(-i\frac{\kappa z}{\mu}\right)\frac{\exp(ikz)}{\mu}\exp\left(-\frac{r^2}{\mu w_0^2}\right)\int_{-\pi}^{\pi} A(\varphi) \times \exp\left[i\left(\frac{k_x x}{\mu}+\frac{k_y y}{\mu}\right)\right]\mathrm{d}\varphi. \tag{A16}$$

From Eq. (3), we note that the integral in Eq. (A16) describes the transverse field distribution W of an ideal nondiffracting beam evaluated at the scaled coordinates $(x/\mu, y/\mu)$. The expression for the HzG beams can be finally rewritten as

$$U(\mathbf{r}) = \exp\left(-i\frac{\kappa z}{\mu}\right)\frac{\exp(ikz)}{\mu}\exp\left(-\frac{r^2}{\mu w_0^2}\right)W\left(\frac{x}{\mu},\frac{y}{\mu};k_t\right), \tag{A17}$$

which is the same as Eq. (4).

APPENDIX B: DERIVATION OF THE ANGULAR SPECTRUM OF THE HELMHOLTZ–GAUSS BEAM

Across a transverse plane z, the field $U(\mathbf{r})$ has the angular spectrum given by the two-dimensional Fourier transform

$$\mathfrak{U}(u,v;z) = \frac{1}{2\pi}\int_{-\infty}^{\infty}\int_{-\infty}^{\infty} U(\mathbf{r})\exp(-ixu - iyv)\mathrm{d}x\mathrm{d}y, \tag{B1}$$

where (u, v) are the Cartesian coordinates in the frequency space. As shown in Appendix A, the field $U(\mathbf{r})$ results from a suitable superposition of fields $u(\mathbf{r})$ [see Eq. (A15)]. Therefore the spectrum $\mathfrak{U}(u, v; z)$ can be found by calculating

$$\mathfrak{U}(u,v;z) = \int_{-\pi}^{\pi} A(\varphi)\mathfrak{F}\{u(\mathbf{r})\}\mathrm{d}\varphi, \tag{B2}$$

where $\mathfrak{F}\{u(\mathbf{r})\}$ is the two-dimensional Fourier transform of $u(\mathbf{r})$. From Eqs. (A14) and (B1), $\mathfrak{F}\{u(\mathbf{r})\}$ is given by

$$\mathfrak{F}\{u(\mathbf{r})\} = f(z)\int_{-\infty}^{\infty}\int_{-\infty}^{\infty}\exp\left(-\frac{r^2}{\mu w_0^2} + \frac{ik_x x}{\mu} + \frac{ik_y y}{\mu} - ixu - iyv\right)\mathrm{d}x\mathrm{d}y, \tag{B3}$$

where $f(z) = \exp(ikz)\exp(-i\kappa z/\mu)\mu^{-1}/2\pi$.

If we write the double integral as the product of two single integrals and apply the known result $\int_{-\infty}^{\infty}\exp(-a^2x \pm bx) = \sqrt{\pi}\exp(b^2/4a^2)/a$, Eq. (B3) becomes

$$\mathfrak{F}\{u(\mathbf{r})\} = D(z)\exp\left(-\frac{w_0^2\mu}{4}\rho^2\right)\exp\left[\frac{w_0^2}{2}(k_x u + k_y v)\right], \tag{B4}$$

where $\rho = (u^2+v^2)^{1/2}$ is the radial coordinate in the frequency space and

$$D(z) = \frac{w_0^2}{2}\exp\left(-\frac{1}{4}k_t^2 w_0^2\right)\exp(ikz) \tag{B5}$$

is an amplitude factor that depends on z only.

Inserting Eq. (B4) into Eq. (B2) and noting from Eq. (3) that the integral

$$\int_{-\pi}^{\pi}\mathrm{d}\varphi A(\varphi)\exp[i(w_0^2 k_x u + iw_0^2 k_y v)/2i] \tag{B6}$$

is the function $W(x, y)$ evaluated at $(w_0^2 u/2i, w_0^2 v/2i)$, we finally obtain

$$\mathfrak{U}(u, v; z) = D(z)\exp\left(-\frac{w_0^2\mu}{4}\rho^2\right)W\left(\frac{w_0^2}{2i}u, \frac{w_0^2}{2i}v; k_t\right), \tag{B7}$$

which is the same as Eq. (10).

APPENDIX C: EXPRESSING THE HELMHOLTZ–GAUSS BEAM IN THE STANDARD NOTATION

For visualization purposes, it is instructive to convert the HzG beam [Eq. (4)] into the standard notation that is widely used in the laser field.[10] If we define the beam width $w(z) = w_0(1 + z^2/z_R^2)^{1/2}$, the radius of curvature $R(z) = z + z_R^2/z$, and the Gouy shift $\Theta(z) = \arctan(z/z_R)$ and also note that $\mu^{-1} = [w_0/w(z)]\exp[-i\Theta(z)]$, the field $U(\mathbf{r})$ takes the form

$$U(\mathbf{r}) = \exp\left(-\frac{r_0^2}{w_0^2}\right)\frac{w_0}{w(z)}\exp\left[-\frac{r^2 - r_0^2}{w^2(z)} + ikz + i\frac{k(r^2 - r_0^2)}{2R(z)} - i\Theta(z)\right]W\left(\frac{x}{\mu}, \frac{y}{\mu}; k_t\right), \tag{C1}$$

where

$$r_0 \equiv \frac{1}{2}k_t w_0^2 = \frac{k_t}{k}z_R. \tag{C2}$$

Note that the amplitude and phase factors accounting for the propagation in Eq. (C1) contain a term that is quadratic in r_0.

The presence of the fundamental Gaussian beam

$$\mathrm{GB}(\mathbf{r}) = \frac{w_0}{w(z)}\exp\left[-\frac{r^2}{w^2(z)} + ikz + i\frac{kr^2}{2R(z)} - i\Theta(z)\right] \tag{C3}$$

as an explicit factor is clearly recognized in expression (C1). The HzG beams can be then written in a more meaningful form as

$$U(\mathbf{r}) = C(z)\mathrm{GB}(\mathbf{r})W\left(\frac{x}{\mu}, \frac{y}{\mu}; k_t\right), \tag{C4}$$

where the complex-amplitude factor $C(z)$ is given by

$$C(z) = \exp\left[\frac{r_0^2}{w^2(z)} - \frac{r_0^2}{w_0^2}\right]\exp\left[-i\frac{kr_0^2}{2R(z)}\right]. \tag{C5}$$

ACKNOWLEDGMENTS

This research was partially supported by Consejo Nacional de Ciencia y Tecnología of México under grant 42808 and by the Tecnológico de Monterrey Research Chair in Optics under grant CAT-007. The authors acknowledge Sabino Chávez for some discussions.

Corresponding author Julio C. Gutiérrez-Vega can be reached by e-mail at juliocesar@itesm.mx. Miguel A. Bandres is also with the Department of Physics and Astronomy, State University of New York at Stony Brook, Stony Brook, New York 11794-3800, and can be reached by e-mail at bandres@gmail.com.

REFERENCES

1. J. Durnin, "Exact solutions for nondiffracting beams. I. The scalar theory," J. Opt. Soc. Am. A **4**, 651–654 (1987).
2. J. Durnin, J. J. Micely, Jr., and J. H. Eberly, "Diffraction-free beams," Phys. Rev. Lett. **58**, 1499–1501 (1987).
3. J. C. Gutiérrez-Vega, M. D. Iturbe-Castillo, and S. Chávez-Cerda, "Alternative formulation for invariant optical fields: Mathieu beams," Opt. Lett. **25**, 1493–1495 (2000).
4. J. C. Gutiérrez-Vega, M. D. Iturbe-Castillo, G. A. Ramírez, E. Tepichín, R. M. Rodríguez-Dagnino, S. Chávez-Cerda, and G. H. C. New, "Experimental demonstration of optical Mathieu beams," Opt. Commun. **195**, 35–40 (2001).
5. S. Chávez-Cerda, M. J. Padgett, I. Allison, G. H. C. New, J. C. Gutiérrez-Vega, A. T. O'Neil, I. MacVicar, and J. Courtial, "Holographic generation and orbital angular momentum of high-order Mathieu beams," Quantum Semiclassic. Opt. **4**, S52–S57 (2002).
6. M. A. Bandres, J. C. Gutiérrez-Vega, and S. Chávez-Cerda, "Parabolic nondiffracting optical wave fields," Opt. Lett. **29**, 44–46 (2004).
7. F. Gori, G. Guattari, and C. Padovani, "Bessel–Gauss beams," Opt. Commun. **64**, 491–495 (1987).
8. Y. Li, H. Lee, and E. Wolf, "New generalized Bessel–Gauss beams," J. Opt. Soc. Am. A **21**, 640–646 (2004).
9. A. P. Kiselev, "New structures in paraxial Gaussian beams," Opt. Spectrosc. **96**, 479–481 (2004).
10. A. E. Siegman, *Lasers* (University Science, Mill Valley, Calif., 1986).
11. I. S. Gradshteyn and I. M. Ryzhik, *Table of Integrals, Series, and Products* (Academic, San Diego, Calif., 2000).